Proceedings of 2004 IEEE/RSJ International Conference on
Intelligent Robots and Systems
September 28 - October 2, 2004, Sendai, Japan

Shape Control of Hyper-Redundant Modularized Manipulator Using Variable Structure Regular Polygon

Jinguo Liu*1*3, Yuechao Wang*1, Shugen Ma*2*1, Bin Li*1
*1. Robotics Laboratory of Chinese Academy of Sciences,Shenyang Institute of Automation (SIA), China
*2. Department of Systems Engineering, Faculty of Engineering, Ibaraki University, JAPAN
*3. Graduate School of Chinese Academy of Sciences, Bejing, China
liujinguo@sia.ac.cn,ycwang@sia.ac.cn,shugen@dse.ibaraki.ac.jp, libin@sia.ac.cn

Abstract—**Hyper-redundant manipulator has more degrees of freedom than the least necessary to perform a given task, thus it has the features of overcoming conventional industrial robot's limitation such as improving its kinematics and dynamic performances. Crucial as it is, effective control of hyper-redundant manipulator is difficult for its redundancy. A novel shape control technique based on the concept of variable structure regular polygon and subsystem has been proposed. This technique, using variable structure regular polygon and neural networks models, is completely capable of solving the control problem of a planar hyper-redundant manipulator with any number of links following any desired path. With regular polygon side number's variety and its shape's transformation, the manipulator's configuration changes accordingly and moves actively to perform the task form point to point or following a path. Compared with other methods to our knowledge, this technique has such superiorities as fewer control parameters, higher precision and less computation. Simulation of a six-link modularized manipulator's inspection work in a bottle-like concave has demonstrated that this control technique is available and effective.**

Keywords—Hyper-redundant manipulator; Inverse kinematics; Neural networks; Shape control; Variable structure regular polygon

I. INTRODUCTION

The hyper-redundant manipulator is defined to have more degrees of freedom than the least necessary to perform a given task. As they have a very large degree of redundancy, hyper-redundant manipulators excel in flexibility, dexterity, versatility and applicability in motion for certain task in a complex environment. The redundancy can be used to overcome the conventional industrial robot's limitation as avoiding singularities, obstacle avoidance or joint limit avoidance. Besides this, the redundancy can be used to optimize the related factors of the manipulator such as path planning, optimizing the joint's displacement, velocity, acceleration, torque, energy and so on. The manipulator has widely application to the structural limited environment, the nuclear radicalized space, the outer space and the deep sea as they can reach behind the obstacle, to grip the objects or crawl into concaves. The merits of hyper-redundant manipulator have focused a lot attention [1]~[11].

As hyper-redundant manipulators have many joints and actuators, it is difficult to solve their inverse kinematics and dynamics problems. But this is the basic step to control the manipulators. In the initial research more attention have been paid to the Jacobian pseudo inverse approach [1][2]. Whereas in this technique there are a lot of matrix computations as the redundancy increases the complexity increases exponentially. Recently many techniques have been proposed to turn the hyper-redundant manipulator into non-redundant manipulators according to the task's need and then solve the subsystems' kinematics and dynamics. Farshid Maghami Asi uses the "virtual link" and "distribution scheme" technique to divide the hyper-redundant manipulator into sub-manipulators such as two-link system and three-link systems[3][4]. R.J. Schilling and F. Fahimi divide the manipulator into proximal section and distal section [4][5]. As they are analogous in shape and operation to snakes, elephant trunks and tentacles, Chirikjian, G. S. has proposed the backbone curve to control the control the hyper-redundant manipulator.[6][7]. Shugen Ma has efficiently controlled the hyper-redundant manipulator by Serpenoid curve [8][9]. Hisato KOBYASHI also adopted the shape control technique to control the continuous manipulator [10]. Whereas the shape control techniques mentioned above are always continuous curve, on the contrary, most manipulators in application are in discrete curves so they are not precise enough to control the hyper-redundant manipulators as during dispersing the curve or integrating the curvature the error is unavoidable [11].

In this paper a new approach has been proposed to control the modularized hyper-redundant manipulators. This technique has been developed to obtain the inverse kinematics solution of the planar hyper-redundant at the position and velocity levels. It is based on the concept variable structure regular polygon and subsystem. Based on neural networks controller, the approach presented in this paper is completely capable of solving the control problem of a planar hyper-redundant manipulator with any number of links following any desired path. Simulation of a six-link modularized manipulator's inspection work in a bottle-like concave has demonstrated that this control technique is available and effective.

II. REPRESENTATION OF PLANAR HYPER-REDUNDANT MODULARIZED MNIPULATOR USING REGULAR POLYGON

A. *Conventioanl Planar Hyper-Reduandant Manipulator*

As shown in Fig.1, the hyper-redundant manipulator has

0-7803-8463-6/04/$20.00 ©2004 IEEE

a lot of links, so it is often repeat and modularized. The manipulator is composed of a serial chain of links with the same length where the internal variables $\theta_i (i = 1 \sim n)$ are the relative angles between adjacent links. The end effector's position is given by

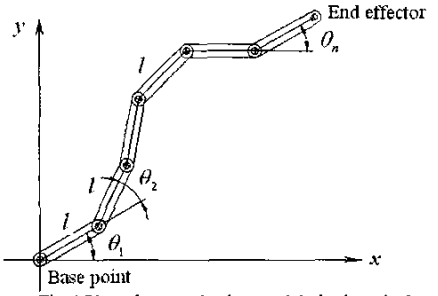

Fig. 1 Planar hyper-redundant modularized manipulator

$$\begin{pmatrix} x \\ y \end{pmatrix} = \left(\sum_{i=1}^{n} l\cos\psi_i, \sum_{i=1}^{n} l\sin\psi_i \right)^T \tag{1}$$

where ψ_i is the absolute link angle given by

$$\psi_i = \sum_{j=1}^{i} \theta_j \tag{2}$$

To control the hyper-redundant manipulator's end effector's position to realize the task as point to point, we have to calculate any joint's relative angle, that is, to solve the inverse problem basically. It is apparent that the equation (1) has indeterminate solutions when $n > 2$. To control the manipulator efficiently it is crucial that the inverse solution should be one and only. Commonly pseudo inverse approach has been used and differentiating equation (1) yields that Jacobian matrix is

$$J = \begin{bmatrix} -\sum_{i=1}^{n} l\sin\psi_i & -\sum_{i=2}^{n} l\sin\psi_i & \cdots & -\sum_{i=n}^{n} l\sin\psi_i \\ \sum_{i=1}^{n} l\cos\psi_i & \sum_{i=2}^{n} l\cos\psi_i & \cdots & \sum_{i=n}^{n} l\cos\psi_i \end{bmatrix} \tag{3}$$

Except when the manipulator is fully extended, J has rank 2 and the joint velocity can be solved by

$$\dot{\theta} = J^T (JJ^T)^{-1} \dot{x} \tag{4}$$

The algorithm's computation increases when the number of the links increases. So in this paper shape control approach has been proposed.

B. Represent the Manipulator Using Regular Polygon

Regular polygon is defined as the polygon has sides with the same length and angles with the same value in plane geometry. As the modularized manipulator has the links with the same length, it is easy for it to pose the configuration like a regular polygon. The hyper-redundant manipulator can be divided into line parts and curve parts. The shape of the curve parts can be controlled by the variable structure regular polygon. The manipulator's shape changes according to the regular polygons' shape shifting or the polygon's sides' change.

As mentioned above, relative angles between adjacent links will have the same value. If we use the regular polygon's shape to control the manipulator, there are fewer variables to deal with and the complexity decreases accordingly. At the same time the redundancy of the manipulator will decrease, the work space and flexibility of the manipulator will lose to some extent. Thus in this paper we use variable structure regular polygon, which means that the number of the regular polygon's sides is variable and the shape of the polygon is variable, instead of using pure regular polygon to control the manipulator. After spreading like a regular polygon, the manipulator possesses enough workspace through manipulator's adaptation, extension and rotation. The hyper-redundant manipulator can be divided into many kinds of subsystems to carry out the task. According to the adjacent links' curvature, the straight subsystems can be looked as long lines and the arc ones can be looked as variable structure regular polygon curves.

To make it easy to describe and calculate, in this paper we define a hyper-redundant manipulator being composed of one arc subsystem P_m and one straight subsystem L_k. P_m represents the above half of a $2m$-link regular polygon and $\overline{P}_m$ the below half. L_k represents a k-link line. $P_{m,i}$ and $L_{k,j}$ represent the i link in the arc subsystem and the j link in the line subsystem from the base point to the end effector respectively. Any manipulator can be spread in such style. For instance a six-link manipulator can be divided into many kinds of $P_m L_k$ or $L_k P_m$ as shown in Fig.2.

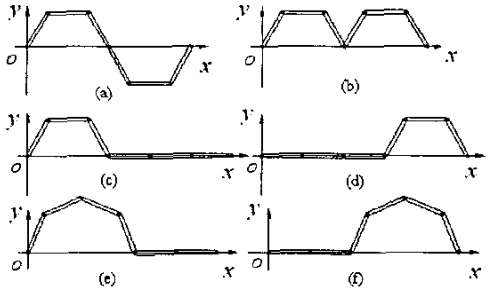

(a) $P_3\overline{P}_3$;(b) P_3P_3; (c) P_3L_3; (d); L_3P_3 (e) P_4L_2; (f) L_2P_4
Fig.2 Spread of six-link manipulator

Any n-link manipulator can spread as N kinds of such configuration. N is given by

$$N = \begin{cases} 2 (n = 2) \\ 4 (n = 3) \\ 4(n-2) + 2 (n \geq 4) \end{cases} \tag{5}$$

The hyper-redundant manipulator can switch between the configurations according to the environment.

III. VARIABLE STRUCTURE REGULAR POLYGON TECHNIQUE

A. Extension and Rotation of P_m

The shape of the manipulator is controlled by P_m's shape which comes from extension and rotation. In this

section, we mainly consider P_m part's configuration, the end effector's position and relative angles of the joints' in P_m. Standard P_m is half of $2m$ -link regular polygon as shown in Fig.3.

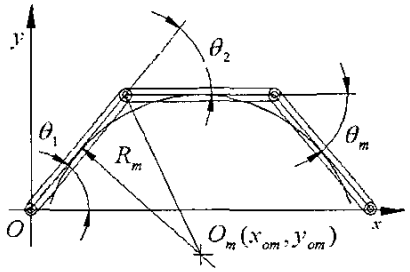

Fig.3 Extension of P_m

To guarantee that the relative angles between adjacent links have the same value and the end effector stays on x -axis. The joint's relative angle can be given by

$$\theta_1 = \frac{m-1}{2m}(1-\alpha)\pi \tag{6}$$

$$\theta_i = \frac{\alpha-1}{m}\pi \ (i = 2 \sim m) \tag{7}$$

where α is the extension coefficient, $-1 \le \alpha \le 1$. And the absolute angle for any joint can be calculated out as

$$\psi_1 = \theta_1 \tag{8}$$

$$\psi_i = \theta_1 + (i-1)\theta_i; \ (i = 2 \sim m) \tag{9}$$

The end effector's position of P_m is given by

$$\begin{pmatrix} x_m \\ y_m \end{pmatrix} = \left(\sum_{i=1}^{m} l\cos\psi_i, \sum_{i=1}^{m} l\sin\psi_i \right)^T \tag{10}$$

where

$$\begin{aligned} x_m &= \sum_{i=1}^{m} l\cos\psi_i \\ &= l(\cos\theta_1 + \cos(\theta_1+\theta_i) + \cdots + \cos(\theta_1 + (m-1)\theta_i)) \\ &= \begin{cases} ml; (\alpha = 1) \\ l\sin(m\theta_i/2)\cos(2\theta_1 + (m-1)\theta_i)/2)/\sin(\theta_i/2); (\alpha \ne 1) \end{cases} \end{aligned} \tag{11}$$

According to θ_1 in (6) and θ_i in e (7), solving equation (9) yields

$$\psi_i = (m/2 + i - 3/2)(\alpha - 1)\pi/m \tag{12}$$

From (11), when $\alpha \ne 1$ the x -axis coordinate of the end effector can be given by

$$\begin{aligned} x_m &= l\sin(m\theta_i/2)\cos((2\theta_1 + (m-1)\theta_i)/2)/\sin(\theta_i/2); \\ &= l\sin((\alpha-1)\pi/2)/\sin((\alpha-1)\pi/2/m) \end{aligned} \tag{13}$$

And

$$\begin{aligned} y_m &= \sum_{i=1}^{m} l\sin\psi_i \\ &= \sin\theta_1 + \sin(\theta_1+\theta_i) + \cdots + \sin(\theta_1 + (m-1)\theta_i) \\ &= \begin{cases} 0; (\alpha = 1) \\ l\sin(m\theta_i/2)\sin((2\theta_1 + (m-1)\theta_i)/2)/\sin(\theta_i/2); (\alpha \ne 1) \end{cases} \\ &= 0 \end{aligned} \tag{14}$$

As shown in Fig.3, geometry topology of inscribed circle of P_m are given by

$$\tan\frac{\pi-\theta_2}{2} = \frac{R_m}{l/2} \tag{15}$$

$$x_{om} = l/2\cos\theta_1 + R_m\sin\theta_1 \tag{16}$$

$$y_{om} = l/2\sin\theta_1 - R_m\cos\theta_1 \tag{17}$$

The radius of the inscribed circle and its center can be given by substituting (6) and (7) into (15), (16) and (17).

$$R_m = \frac{l}{2}\tan\left(\frac{m-\alpha+1}{2m}\pi\right) \tag{18}$$

$$\begin{aligned} x_{om} &= l/2\cos\left(\frac{m-1}{2m}(1-\alpha)\pi\right) \\ &\quad + R_m\sin\left(\frac{m-1}{2m}(1-\alpha)\pi\right) \end{aligned} \tag{19}$$

$$\begin{aligned} y_{om} &= l/2\sin\left(\frac{m-1}{2m}(1-\alpha)\pi\right) \\ &\quad - R_m\cos\left(\frac{m-1}{2m}(1-\alpha)\pi\right) \end{aligned} \tag{20}$$

Results of R_m, x_{om} and y_{om} are used to carry out a grip work or avoiding a round obstacle. The workspace of P_m can be enlarged by combining extension through α 's change and rotation at the base point. After a θ_{rm} rotation of P_m, the end effector's position changes into

$$\begin{pmatrix} x_{rm} \\ y_{rm} \end{pmatrix} = \begin{pmatrix} \cos\theta_{rm} & -\sin\theta_{rm} \\ \sin\theta_{rm} & \cos\theta_{rm} \end{pmatrix} \begin{pmatrix} x_m \\ y_m \end{pmatrix} \tag{21}$$

The inscribed cycle's position changes accordingly.

$$\begin{pmatrix} x_{rom} \\ y_{rom} \end{pmatrix} = \begin{pmatrix} \cos\theta_{rm} & -\sin\theta_{rm} \\ \sin\theta_{rm} & \cos\theta_{rm} \end{pmatrix} \begin{pmatrix} x_{om} \\ y_{om} \end{pmatrix} \tag{22}$$

As shown in Fig.4, the length of links is 1 and the 4-link manipulator's configuration and its inscribed circle's position can change through rotation and extension. The inscribed circle can be considered as a round object for grip or avoid.

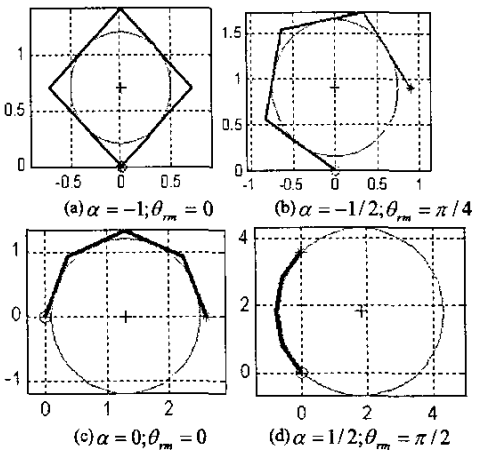

Fig. 4 Extension and rotation of P_4

B. Inverse Kinematics of P_m

In planar coordinate the inverse kinematics of P_m is given by

$$(\alpha, \theta_{rm}) = f(x_m, y_m, m) \tag{23}$$

where the relations between α , θ_{rm} and x_m, y_m are

$$\theta_{rm} = \tan 2^{-1}(y_m / x_m) \tag{24}$$

$$r_m = \sqrt{x_m^2 + y_m^2} \tag{25}$$

From (13) the length of the vector from the base point to the end effector is given by

$$r_m = l \sin((\alpha - 1)\pi / 2) / \sin((\alpha - 1)\pi / m / 2) \tag{26}$$

When the hyper-redundant manipulator carries out a work, continuous change of the velocity is very important. Direct kinematics of extension and rotation includes the planning of $\dot{\theta}_{rm}$ and $\dot{\alpha}$ .Firstly the velocity has been limited by the mechanism in practical application. Second the velocity must be continuous. As the motion of any rotation or extension is step by step, the initial velocity and the final velocity are planned to be zero.

If P_m only extends, α is given by

$$\alpha(t) = \alpha_{ei} + (\alpha_{ef} - \alpha_{ei}) \times (1 + \sin((t - t_{ei})\pi / (t_{ef} - t_{ei}) - \pi / 2)) / 2 \tag{27}$$

where α_{ei} is initial α , α_{ef} is final α , t_{ei} is initial time, t_{ef} is final time during extension respectively. In (27), it is guaranteed that $\dot{\alpha}(t)$ is zero at the initial and the final time of an extension stage.

Through differential of equation (6) and (7), we get

$$\dot{\theta}_1 = \dot{\alpha}\pi / (2m) \tag{28}$$

$$\dot{\theta}_i = \dot{\alpha}\pi / m \ (i = 2 \sim m) \tag{29}$$

From (31) and (32), we can see that

$$\dot{\alpha}_{\max} \le 2m\dot{\theta}_1 / \pi \tag{30}$$

$$\dot{\alpha}_{\max} \le m\dot{\theta}_{i\max} / \pi \ (i = 2 \sim m) \tag{31}$$

where $\dot{\theta}_{i\max}$ is the maximum velocity of the joint from 2 to m and is limited by the mechanism of the hyper- redundant manipulator. So the time $t_{ef} - t_{ei}$ in (27) is limited by mechanism performance and relative change of α , the function is

$$t_{ef} - t_{ei} = \beta \frac{a}{\dot{\theta}_{\max}} \tag{32}$$

where β is performance coefficient decided by manipulator's mechanism.

If P_m only rotates, θ_{rm} changes and α doesn't change. We plan θ_{rm} instead.

$$\theta_{rm}(t) = \theta_{ei} + (\theta_{ef} - \theta_{ei}) \times (1 + \sin((t - t_{ei})\pi / (t_{ef} - t_{ei}) - \pi / 2)) / 2 \tag{33}$$

where θ_{ei} is initial θ_{rm} , θ_{ef} is final θ_{rm} , t_{ei} is initial time and t_{ef} is final time during rotation respectively. In (33), it is guaranteed that $\dot{\theta}_{rm}(t)$ is zero at the initial and the final time of a rotation stage.

When both extension and rotation exist, the velocities of the manipulator joints are given by

$$\dot{\theta}_1 = \frac{d\theta_1}{d\alpha}\frac{d\alpha}{dt} + \frac{d\theta_{rm}}{dt} \tag{34}$$

$$\dot{\theta}_i = \frac{d\theta_i}{d\alpha}\frac{d\alpha}{dt} \ (i = 2 \sim m) \tag{35}$$

where $d\alpha / dt$ and $d\theta_{rm} / dt$ come from planning the extension and rotation mentioned in (27) and (33). In the same way, the angle acceleration also can be calculated from differential of (34) and (35).

It can be seen from the process that the inverse kinematics solution of P_m exists and is sole. We cannot yield the result easily from solving the equations from (23) to (35) because of their nonlinearity and trigonometric function often has a lot of solutions, so it is hard to choose the satisfied one. For a n-link modularized manipulator, the link of P_m can change from 2 to n, so there are n-1 group of nonlinear functions existing.

In recently years, neural networks (NNs)'s application in robotics has focused a lot attention. The nonlinear mapping and learning properties of NNs are key factors for their use in intelligent control field and nonlinear optimization. The learning capability of NNs is used to make the controller learn a certain function, highly nonlinear, represent the direct kinematics and dynamics, inverse kinematics and dynamics or any other characteristics of the system. This is usually performed during a normally long training period when commissioning the NNs controller in a supervised or unsupervised manner [12]~[13]. More about the principle of NNs has been depicted clearly in [13]~[15].

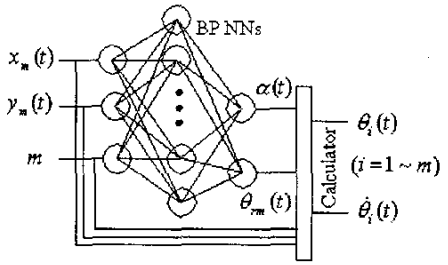

Fig.5 Neural networks controller

A three-layered error back-propagation (BP) controller model, as shown in Fig.5, has been proposed to solving the inverse kinematics of (23)~(35). BP algorithm is a supervised learning by back propagating the model's error to meet the need step and step. For a n-link modularized hyper-redundant manipulator, the data of the direct inverse kinematics of manipulator from 2-link to n-link has been used to training the model offline firstly. As shown in Fig.5, for any n-link hyper-redundant manipulator, we use $m = 2 \sim n$, $\alpha = -1 : 0.01 : 0.99$, $\theta_{rm} = 0 \sim 2\pi$ and $l = 1$ to train the neural network offline. The model includes a calculator following the output of neural networks. This calculator which

synthesizes the equations as (6),(7),(34)and (35) has been developed for calculate the relative angles and velocities. The acceleration of the joints also is available. This model can be used online and in real time control.

For instance, the manipulator P_3's end effector has to follow a circle path in three seconds, as shown in Fig.6 (a). The length of the link is 1m, the circle's radius is 0.5m and the center coordinates of the circle are (1,1). We plan the changing of the end effector's position as

$$x_m(t) = 1 + 0.5\cos(\phi(t)) \quad (36)$$

$$y_m(t) = 1 + 0.5\sin(\phi(t)) \quad (37)$$

$$\phi(t) = (1 + \sin(t\pi/3 - \pi/2))\pi \quad (38)$$

It is shown that the NNs controller has high precision in the simulation and both the velocities and accelerations are continuous. Especially, the initial and final of the angle velocities and accelerations are zero.

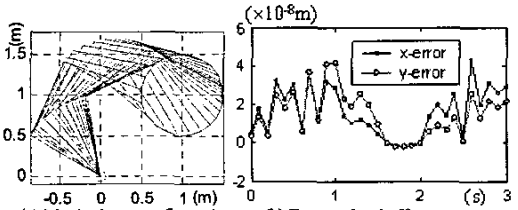

(a) Manipulator configurations (b) Errors of end effector

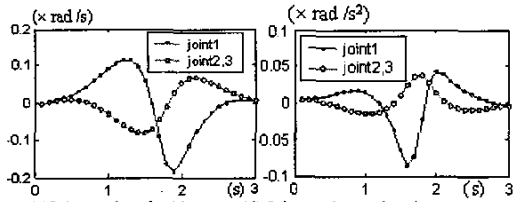

(c)Joint angle velocities (d) Joint angle accelerations

Fig.6 Example of P_3's contour motion

C. P_mL_k's Variable Structure Algorithms

As mentioned previously, structure's change of the hyper-redundant manipulator can be used to improve the robot's flexibility to meet the practical requirement. This configuration changes from the decrease or increase of m and k. The end effector vector of P_mL_k is given by

$$\vec{r}_n = \vec{r}_m + \vec{r}_k \quad (39)$$

where $\vec{r}_s$ is decided by the length of link l ,the number of links m ,the extension coefficient α and the rotation of $P_m - \theta_{rm}$, $\vec{r}_k$ is decided by the length of link l ,the number of links k , θ_{rm} and the relative rotation of L_k from $P_m - \theta_{rk}$. So the end effector's vector can be given by

$$\vec{r}_n = \vec{r}_m + \vec{r}_k = \begin{pmatrix} \cos\theta_{rm} & -\sin\theta_{rm} \\ \sin\theta_{rm} & \cos\theta_{rm} \end{pmatrix} \left(\begin{pmatrix} x_m \\ y_m \end{pmatrix} + \begin{pmatrix} kl\cos\theta_{rk} \\ kl\sin\theta_{rk} \end{pmatrix} \right) \quad (40)$$

where x_m and y_m come from (13) and (14).

There are two kinds of basic structure change such as $P_mL_k \to P_{m+1}L_{k-1}$ and $P_mL_k \to P_{m+1}L_{k-1}$. In this paper we only consider the former process as the later is the inverse of the former.

The algorithm of manipulator carrying out a task and structure changing from P_mL_k to $P_{m+1}L_{k-1}$ can be generalized as following:

1) Judge if P_mL_k can perform the task or not, if not continue the structure change, else rotate or extend P_mL_k;
2) Describe the initial configuration P_mL_k;
3) Describe the initial configuration $P_{m+1}L_{k-1}$;
4) Differentiate the static and the moving links;
5) Set the $m+1$ link's distal end as the base point and this link rotates around the base point from initial configuration to final configuration;
6) Rotation and extension of P_m to follow the change of the $m+1$ link's proximal end till P_{m+1} comes into being;
7) $m=m+1$, $k=k-1$, go to step 1).

In this algorithm step 6 is the most important step and is similar with the inverse kinematics of P_m. It has been demonstrated in Fig.7 that the manipulator changes from P_5L_2 into P_6L_1 in two seconds. The length of the link is 1m. Both at the initial stage and the finial stage: $\theta_{rm} = 0, \theta_{rk} = 0$ .We plan the changing of P_5's end as

$$x_5(t) = 2.5 + \cos(\phi(t)) \quad (41)$$

$$y_5(t) = 2.5 + \sin(\phi(t)) \quad (42)$$

$$\phi(t) = \pi + (1.3861 - \pi)(1 + \sin(t\pi/2 - \pi/2))/2 \quad (43)$$

Simulation result has been shown in Fig.7

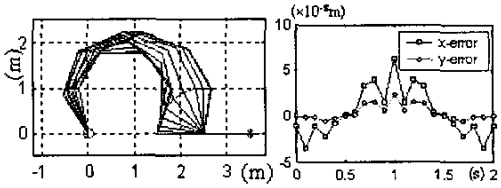

(a) Manipulator configurations (b) Errors of end effector

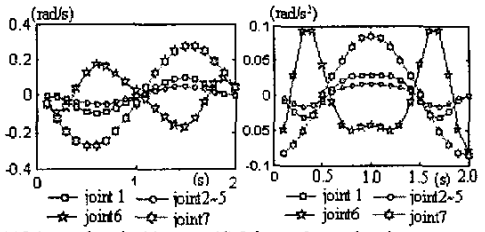

(c)Joint angle velocities (d) Joint angle accelerations

Fig.7 Example of $P_5L_2 \to P_6L_1$

IV. SIMULATION

As mentioned previously, hyper-redundant manipulator has several potential advantages over non-redundant manipulator. The extra degrees of the freedom can be used to achieve some special goals such as

singularity avoidance, obstacle avoidance or joint limit avoidance. In a workspace with obstacle it can move around or between obstacles and thereby to manipulate in situations that otherwise would be inaccessible.

As shown in Fig.8, a six-link modularized manipulator carries out an inspection work into a bottle-like concave through rotation, extension and structure variable step by step.

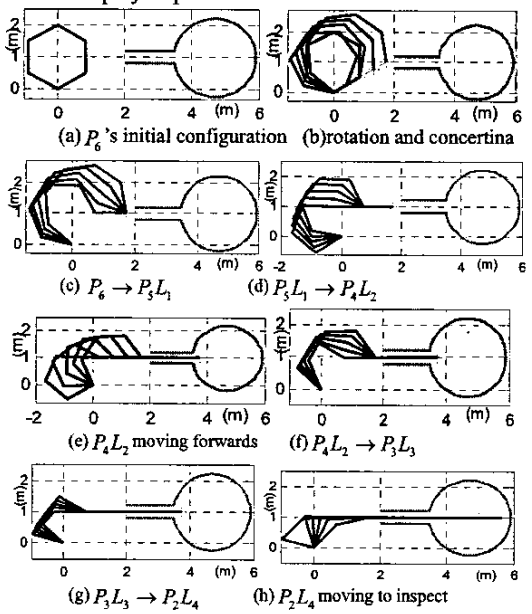

Fig. 8 Simulation of an inspection task

The length of the link is 1m and the every stage 3 seconds is consumed. In the initial configuration, the 6-link modularized manipulator has a pose like a regular hexagon. And then it changes its configuration to crawl into the bottle-like concave. The configurations in this process are shown in details from Fig.8 (b) to Fig.8 (h). Whereas the velocities and accelerations of the manipulator joints are not provided as they have the same performances as in Fig6.and Fig7.

V. CONCLUSIONS

In this paper a new technique has been proposed to control the hyper-redundant modularized manipulators. This technique has been developed to obtain the inverse kinematics solution of the planar hyper-redundant at the position and velocity levels. The hyper-redundant manipulator can be divided into line parts and curve parts. The shape of the curve parts can be controlled by the variable structure regular polygon. The manipulator's shape changes by the regular polygon's shape variety or the polygon's side's variety. The approach presented in this paper is completely capable of solving the control of a planar hyper-redundant manipulator with any number of links following any desired path. The efficiency of the algorithm has been improved by using compound neural networks. And this shape control approach is demonstrated by solving the inverse kinematics problem for robots with six links carrying out the inspection work into a bottle-like concave. This control technique can be used in more complicated environment. And the algorithm should be optimized according to the actual need. When the joint increases, joint torque will increase quickly. How to make it work well in practice is desired in the future.

ACKNOWLEDGMENT

This research is supported partly by China National 863 Program No.2001AA422360.

REFERENCES

[1] R.P. Podhorodeski, A. A.goldenberg, R.G. Fenton . "Resolving redundant manipulator joint rates and identifying special arm configurating using jacobian null-space bases," IEEE TARNSACTION ON ROBOTICS AND AUTOMATION, Vol.7, No.3, 1991, pp.607-618

[2] CHARLES A. KIEIN, CHING-HSIANG HUANG "Review of Pseudoinverse Control for Use with Kinematically Redundant Manipulators," IEEE TARNSACTION ON SYSTEM,MAN AND CYBERNETIC, Vol. SMC-13,No. 3, 1983, pp.245-250

[3] Farshid Maghami Asi, Hashem Ashrafiuon, C. Nataraj . "A General Solution for the Position, Velocity and Acceleration of Hyper-redundant Planar Manipulators," Journal of Robotic System 19(1), 2000, pp. 1-12

[4] F. Fahimi, H. Asrafiuon, C. Nataraj. "Obstacle Avoidance for Spatial Hyper-redundant Manipulators Using Harmonic Potential Functions and the Mode Shape Technique," Journal of Robotic System 20(1), 2003, pp.23-33

[5] R.J. Schilling, R. Read, V. Lovass-Nagy etc. "Path Tracking with the Links of a Planer Hyper-Redundant Robotic Manipulator," Journal of Robotic System 12(3), 1995, pp.189-197

[6] Chirikjian, G. S.,Burdick, J.W., "an obstacle avoidance algorithm for hyper-redundant manipulators," ICRA1990, pp.625-631

[7] Chirikjian, G. S.,Burdick, J.W, "the kinematics of hyper-redundant robot locomotion," IEEE TARNSACTION ON ROBOTICS AND AUTOMATION,Vol.11,No.6, 1995, pp.781-793 .

[8] Shugen Ma, Shigeo Hirose, Hiroshi Yoshinada. "Development of a Hyper-Redundant Multijoint Manipulator for Maintenance of Nuclear Reactors," Advanced Robotics, Vol.9, No.3, 1995, pp.281-300

[9] Shugen Ma, Mototsugu Konno. "An Obstacle Avoidance Scheme for Hyper-redundant Manipulators –Global Motion Planning in Posture Space," ICRA 1997, pp.161-166

[10] Hisato KOBYASHI, Shigeo OHTAKE. "Shape Control of Hyper Redundant Manipulator," ICRA 1995,pp.2803~2808

[11] H. Mochiyanam, E. Shimemural, H. Kobayashi. "Control of manipulators with hyper degrees of freedom: shape tracking based on curve parameter estimation," ICRA1997, pp.173~178

[12] Hecht-Nielsen R. "Theory of the backpropagation neural networks," Proc. of the International Joint Conference on Neural Networks. 1989(1), pp.593-611

[13] H.Daniel Patino, BenjaminR. Kuchen. "Neural networks for advanced control of robot manipulators," IEEE TRANSCATION ON NEURAL NETWORKS, Vol.13, No.2, 2002, pp.343-354

[14] Yunong Zhang, Jun Wang, Youshen Xia. "A dual neural network for redundant resolution of kinematically redundant manipulators subject to joint limits and joint velocity limits," IEEE TRANSCATION ON NEURAL NETWORKS. Vol. 14, No.3, 2003, pp.658~667

[15] A.S. Morris, A. Mansor. "Finding the inverse kinematics of manipulators arm using artificial neural network with lookup table," Robotica, Vol.15, 1997, pp.617-625